

GIGACYCLE FATIGUE BEHAVIOR OF CAST ALUMINUM IN TENSION AND TORSION LOADING

Xue Hongqian¹, Wu Tieying², Bathias C³

- (1. School of Mechanical Electronic, Northwestern Polytechnical University, Xi'an, 710072, P. R. China;
2. College of Energy and Power Engineering, NUAA, 29 Yudao Street, Nanjing, 210016, P. R. China;
3. Laboratory of Energy and Energy Conservation, Paris X University, Ville D'avray, 92410, France)

Abstract: An improved understanding of fatigue behavior of a cast aluminum alloy (2-AS5U3G-Y35) in very high cycle regime is developed through the ultrasonic fatigue test in axial and torsion loading. The new developed torsion fatigue system is presented. The effects of loading condition and frequency on the very high cycle fatigue (VHCF) are investigated. The cyclic loading in axial and torsion at 35 Hz and 20 kHz with stress ratio $R = -1$ is used respectively to demonstrate the effect of loading condition. $S-N$ curves show that the fatigue failure occurs in the range of 10^5-10^{10} cycles in axial or torsion loading and the asymptote of $S-N$ curve is inclined, but no fatigue limit exists under the torsion and axial loading condition. The fatigue fracture surface shows that the fatigue crack initiates from the specimen surface subjected to the cyclic torsion loading. It is different from the fatigue fracture characteristic in axial loading in which fatigue crack initiates from subsurface defect in very high cycle regime. The fatigue initiation is on the maximum shear plane, the overall crack orientation is on a typical spiral 45° to the fracture plane and it is the maximum principle stress plane. The clear shear strip in the torsion fatigue fracture surface shows that the torsion fracture is the shear fracture.

Key words: fatigue testing; torsion fatigue; very high cycle fatigue (VHCF); torsion loading; cast aluminum

CLC number: TG146.21;O346.2

Document code: A

Article ID: 1005-1120(2011)01-0032-06

INTRODUCTION

AS5U3G-Y35 aluminum alloy is highly suitable for high strength cast alloys due to its good flowability of melt and high strength^[1]. The use of the cast aluminum alloys in automotive or aircraft structural applications is rapidly growing to reduce weight. The aluminum alloy also has the low thermal conductivity and the excellent corrosion resistance which makes it favorable in aircraft engine structural applications.

For aluminum alloys applied to aircraft engine components, there is a need for understanding the fatigue behavior of alloys in the very high cycle regime. Ultrasonic fatigue instrumentation at frequency of 20 kHz was used to reduce testing time and examine very long life fatigue behav-

ior^[2-5], which validated that it was an effective and reliable way to investigate fatigue properties of materials^[5-8]. However, much of the available ultrasonic fatigue properties today are axial loading, although some fatigue criterions can be used to predict the torsion fatigue behavior using the axial fatigue life^[9-10]. Because many components are primarily under torsion loading conditions, the investigation of fatigue behavior for the cast aluminum extends a wider range of test conditions involving axial and torsion loading to understand the fatigue properties and the damage mechanisms of the material beyond 10^{10} cycles.

In this paper, samples of cast aluminum are used for fatigue test in the axial and torsion loading at 35 Hz and 20 kHz, respectively. The fa-

Foundation items: Supported by the National Natural Science Foundation of China (50775182); the Scientific Research Foundation for the Returned Scholars of the Ministry of Education of China.

Received date: 2010-10-18; **revision received date:** 2011-01-10

E-mail: xuedang@nwpu.edu.cn

tigue strength and the fracture mechanism of each specimen are also investigated. And the relationship of fatigue strength between in axial loading and torsion loading is discussed.

1 EXPERIMENTS

1.1 Material

The material examined in this paper is 2-AS5U3G-Y35 cast aluminum alloy. The chemical composition is measured by the energy dispersed X-ray spectrometry (EDXS). The results are listed in Table 1, and typical values of mechanical properties are exhibited in Table 2, where E is the Young's modulus, ρ the density, A the reduction in area, σ_y the uniaxial yield stress, UTS the ultimate strength, and HV30 the hardness. The microstructure of cast aluminum 2-AS5U3G-Y35 is shown in Fig. 1. The average grain is $10\ \mu\text{m}$, and a little fine pore (no more than $5\ \mu\text{m}$) is finely dispersed in the microstructure. Solid cylindrical specimens are used with a gauge section of 5 mm in diameter.

Table 1 Chemical composition (in mass) of cast aluminum 2-AS5U3G-Y35

Chemical element	Si	Mn	Ni	Cu	Mg	Fe	Zn	Ti	Pb	Sn
Mass ratio	5.30	0.30	0.03	3.20	0.36	0.55	0.17	0.11	0.02	0.01

Table 2 Mechanical properties of cast aluminum 2-AS5U3G-Y35

E / GPa	ρ / ($\text{kg} \cdot \text{m}^{-3}$)	A / $\%$	σ_y / MPa	UTS/ MPa	HV30
72	2 700	1	182	222	98.6

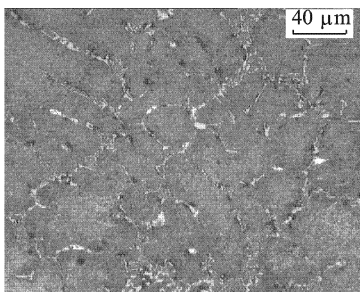


Fig. 1 Microstructure of cast aluminum 2-AS5U3G-Y35

1.2 Fatigue testing method

Fatigue tests are conducted in an ultrasonic fatigue testing machine under the axial or torsion loading at the frequency of 20 kHz. In the ultrasonic fatigue testing, the specimens are cooled by using the compressed air to decrease the temperature of the testing specimen. And fatigue tests are performed until the failure of a specimen, or up to 10^{10} cycles as run-out. The experimental results are compared with the results obtained at the frequency of 35 Hz using conventional fatigue test machine.

1.3 Ultrasonic fatigue test system for torsion loading

Ultrasonic fatigue test system in axial loading is widely used in the fatigue behavior investigating of material in very high cycle regime^[2-6]. In order to test the fatigue behavior of materials subjected to cyclic torsion loading to 10^{10} cycles, an ultrasonic torsion fatigue system is designed based on the ultrasonic fatigue system in the axial loading.

In the ultrasonic torsion fatigue test system, the torsion amplifier that transforms the longitudinal vibration to the torsion vibration and the output amplified by the torsion angular displacement is used to supply the shear stress to the specimen. The torsion vibration system is comprised of a converter, a longitudinal amplifier, a torsion amplifier, and a torsion specimen (Fig. 2). The torsion amplifier and the specimen have the 20 kHz torsion resonance length, and the torsion displacement amplitude of the specimen reaches its maximum in the end, while the shear strain excitation attains the maximum in the middle section of the specimen producing the required high frequency fatigue shear stress.

In this paper, all tests are performed at the stress ratio of $R = -1$. Prior to the each test, the strain in the center (the maximum strain site) of specimen is calibrated with a strain gage bonded to the gage section. Under the nominal elastic conditions used for loading to very high cycles,

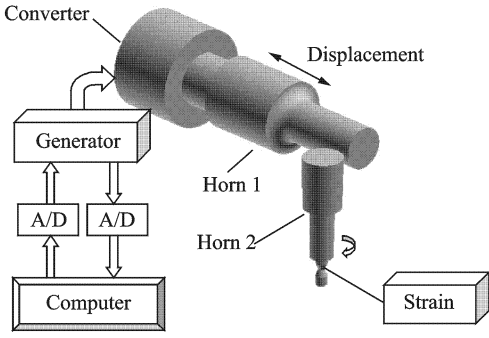


Fig. 2 Ultrasonic torsion fatigue setup

there is a linear relationship between the input voltage and the strain in the gage section. A signal amplifier and an oscilloscope are used to measure strain in the gage section. The computerized control unit allows switching from input voltage to stress control during a running test. Cyclic numbers, maximum stress and testing frequency are continuously recorded by the test control software.

1.4 Dynamic analysis

The difference of ultrasonic fatigue test system between in the axial loading and in the torsion loading is that a torsion amplifier is used to supply the torsion angular displacement to the torsion specimen. In order to obtain a reasonable vibration model of the ultrasonic torsion test system, the ultrasonic test setup is modeled by using the finite element software ANSYS. The dynamic vibration displacement analysis of the system is shown in Fig. 3, and the maximum torsion displacement at the end of torsion amplifier can be seen from the figure.

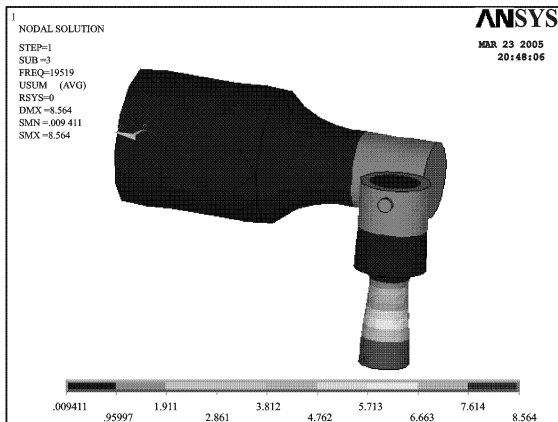


Fig. 3 Displacement field in torsion system

2 RESULTS AND DISCUSSION

2.1 High-cycle fatigue properties

Fatigue tests are divided into two kinds of loading type: one is uniaxial tension-compression fatigue with $R = -1$; another is torsion fatigue with $R = -1$. Prior to fatigue tests, all specimens are polished and the roughness of specimen is less than $0.2 \mu\text{m}$, which satisfied the ASTM standard of metallic materials fatigue test.

Conventional fatigue tests (35 Hz) are conducted by the INSTRON fatigue test machine, in which the cycle stress loading is controlled. The fatigue test results are between 10^4 and 10^7 cycles, and by using the ultrasonic fatigue test machine, the 10^5 – 10^{10} cycles fatigue data are obtained.

The results from the ultrasonic fatigue test system compared with the results obtained using conventional testing machines are plotted together in Fig. 4 ($R = -1$). The results show that many specimens failed in the range of 10^7 – 10^{10} cycles. There is no endurance limit existed in the S - N curve of 2-AS5U3G-Y35, and the S - N curve continues to decrease from 10^7 to 10^{10} cycles.

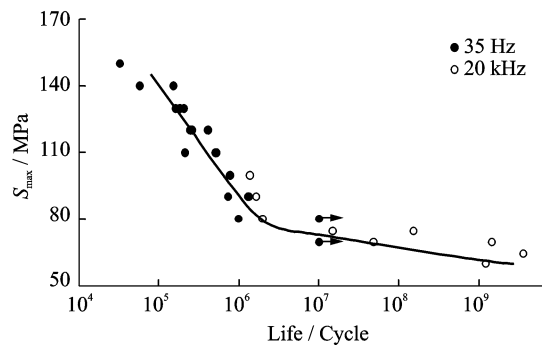


Fig. 4 Experimental results of 2-AS5U3G-Y35 in axial loading ($R = -1$)

Fig. 5 shows the S - N curve of cast aluminum 2-AS5U3G-Y35 for torsion fatigue test with $R = -1$. In Fig. 5, the fatigue lifetime increases as the stress amplitude decreases in the life range of 10^4 – 10^7 cycles, and the fatigue fracture occurs beyond 10^7 cycles. However, the slope of S - N curve decreases a little.

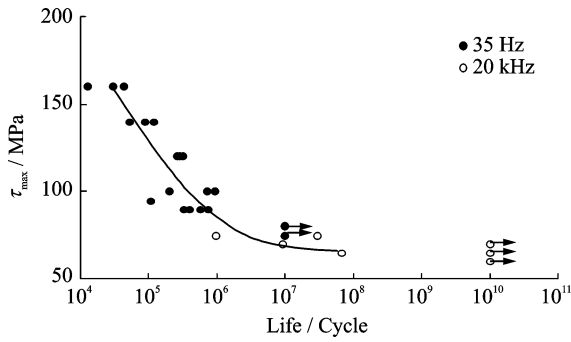


Fig. 5 Torsion fatigue test results of 2-AS5U3G-Y35 ($R = -1$)

2.2 Fatigue fracture mechanism

The fatigue crack initiations of most fractured specimens in the axial loading are from the surface or the subsurface voids in the specimens. Fig. 6 shows a typical fatigue fracture surface tested at 20 kHz and an applied maximum stress level of 70 MPa. The topography of the fracture surfaces are found to obtained the void at the subsurface of specimen. In the vicinity of crack origin, a zone with a number of pores exists. Fig. 7 shows the subsurface fatigue crack initiation tested at the frequency of 20 kHz with the same applied maximum stress level of 70 MPa. Compared with the fatigue fracture surface in Fig. 6, a larger void is in the crack origin. So it has shorter fatigue life with $N_f = 4.47 \times 10^7$ cycles than that of the fractured specimen with $N_f = 1.46 \times 10^9$ cycles shown in Fig. 6.

Observed cracks in the torsion fatigue specimens appear on the maximum shear planes. Although in the some cases the overall crack orientation appears on a typical spiral 45° fracture plane (i. e., maximum principal stress plane),

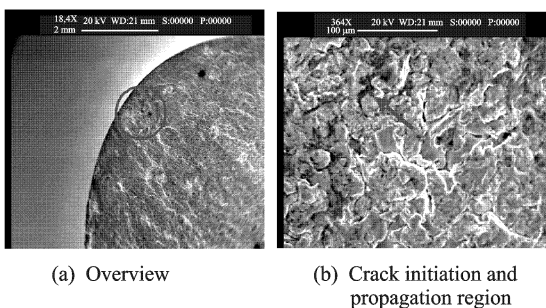


Fig. 6 Subsurface fatigue crack initiation of specimen tested with $N_f = 1.46 \times 10^9$ at 20 kHz

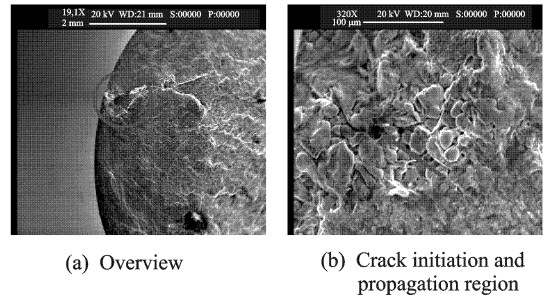


Fig. 7 Subsurface fatigue crack initiation of specimen tested with $N_f = 4.47 \times 10^7$ at 20 kHz

the fatigue damage mechanism is actually shear. Fatigue crack initiations of all the fractured specimens are from surface of specimens. Fig. 8 shows a typical torsion fatigue fracture surface. For the fatigue crack growth in the 45° of axial direction, there are micro-cracks around the principal crack. The fatigue crack growth reveals the spiral 45° fracture plane and the fatigue initiation is from the specimen surface.

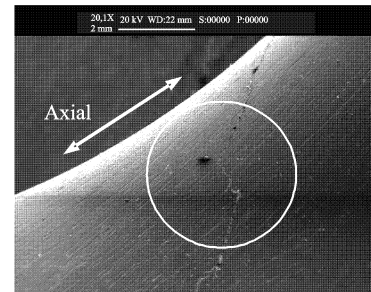


Fig. 8 Growth of torsion fatigue crack

2.3 Discussion

2.3.1 Prediction of shear fatigue properties

Predictions of the torsional fatigue behavior are obtained by using the axial fatigue life data. The shear fatigue properties in the torsional strain-life equation are calculated based on von Mises, Tresca and maximum principal strain criteria respectively. According to the von Mises criterion^[11], we have

$$\tau'_f = \sigma'_f / \sqrt{3}, \quad \gamma'_f = \sqrt{3} \epsilon'_f \quad (1)$$

For the Tresca criterion, we have

$$\tau'_f = \sigma'_f / 2, \quad \gamma'_f = 1.5 \epsilon'_f \quad (2)$$

And for the maximum principal strain criterion, we have

$$\tau'_f = \sigma'_f / (1 + \nu), \quad \gamma'_f = 2 \epsilon'_f \quad (3)$$

The curve of shear stress amplitude versus the fatigue life from experiments and predictions is shown in Fig. 9. It can be seen that among the three criteria, the maximum principal strain criterion provides the best estimation of the torsional fatigue behavior. However, none of these criterion results is in a satisfactory prediction. Choosing the Tresca criterion can lead to very poor predictions and a conservative design.

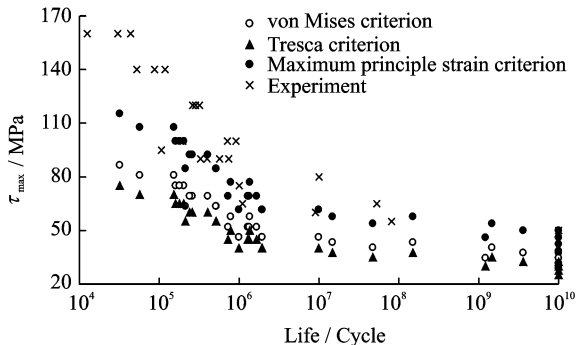


Fig. 9 Results of experiments and predictions

2.3.2 Torsion fatigue mechanism in high cycle regime

Under a cyclic torsional loading condition, the fatigue crack initiates from surface of the specimen center subjected to the maximum shear stress. When the fatigue crack initiates, the local stress raises and different stress states exist around the fatigue crack initiation. The tensile stress on the 45° plane exceeds the tensile strength of the alloy before the shear stress reaches the shear strength. The fracture occurs normal to the 45° tensile plane, thus forming a conical fracture surface.

As the loading is axially symmetrical, a fatigue crack can be initiated at any point, or at several points in the center of specimen which shows the maximum shear stress. The multiple cracks do not occur in the same plane and are separated from each other.

It is discovered from examination of fatigue fracture surface that the fracture surface contains the evident shear fatigue strip and the fatigue cracks arising from torsional stresses show beach marks, although in some cases the overall crack orientation appears on a typical spiral 45° frac-

ture plane (i. e., maximum principal stress plane). It is also found that the fatigue damage mechanism is in fact shear.

The growth cracks are oriented at approximately 45° to the axis of specimen, which indicates that the final fracture is caused by a tensile stress normal to the 45° plane, and unlike the expectation of the shear stress causing an overload failure.

3 CONCLUSIONS

From the investigation of fatigue properties of the cast aluminum 2-AS5U3G-Y35 in a very high cycle regime, the following conclusions can be drawn:

(1) Fatigue failure occurs in the very high cycle regimes for the cast aluminum alloy without fatigue limits and evident frequency effect. The fatigue criterions cannot be used in prediction of torsion fatigue strength using axial fatigue life data.

(2) High cycle fatigue lives are pronounced and determined by fatigue crack initiation. The different fatigue initiation occurs under the different loading condition. For the specimens in the axial loading in high cycle regimes, fatigue crack initiations are often from subsurface or interior defect. Fatigue strength strongly depends on casting defects. If there is no evident microstructure defect, the fatigue crack initiation is also from the specimen surface.

(3) Fatigue crack always initiates from the specimen surface for the torsion fatigue test. The growth cracks are oriented at approximately 45° to the axis of specimen, which indicates that the final fracture is caused by a tensile stress normal to the 45° plane and it is not the expected shear stress causing an overload failure.

References:

- [1] Wang Qingyuan, Berand J Y, Bathias C. Gigacycle fatigue of ferrous alloys[J]. *Fatigue & Fracture of Engineering Materials & Structures*, 1999, 22(8): 667-672.

- [2] Mayer H, Papakyriacou M, Zettl B, et al. Influence of porosity on the fatigue limit of die cast magnesium and aluminium alloys [J]. *International Journal of Fatigue*, 2003, 25(3):245-256.
- [3] Sun Zende, Bathias C, Baudry G. Fretting fatigue of 42CrMo4 steel at ultrasonic frequency [J]. *International Journal of Fatigue*, 2001, 23(5):449-453.
- [4] Bathias C. There is no infinite fatigue life in metallic materials [J]. *Fatigue & Fracture of Engineering Materials & Structures*, 1999, 22(7):559-565.
- [5] Murakami Y, Nomoto T, Ueda T. Factors influencing the mechanism of superlong fatigue failure in steels [J]. *Fatigue & Fracture of Engineering Materials & Structures*, 1999, 22(7):581-590.
- [6] Bayraktar E, Bathias C, Xue Hongqian, et al. On the giga cycle fatigue behaviour of two-phase ($\alpha_2 + \gamma$) TiAl alloy [J]. *International Journal of Fatigue*, 2004, 26(2):1263-1275.
- [7] Xue Hongqian, Tao Hua, Bathias C. The analysis of specimen design for fatigue test at ultrasonic frequency [C] // The 3rd International Conference on Very High Cycle Fatigue. Tokyo, Japan: [s. n.], 2004:440-447.
- [8] Bayraktar E, Marines I, Bathias C. Failure mechanisms of automotive metallic alloys in very high cycle fatigue range [C] // Proceeding of the Third International Conference on Very High Cycle Fatigue. Toyko, Japan: [s. n.], 2004:124-131.
- [9] Davoli P, Bernasconi A, Filippini M, et al. Independence of the torsional fatigue limit upon a mean shear stress [J]. *International Journal of Fatigue*, 2003, 25(6):471-480.
- [10] Murakami Y, Takahashi K. Torsional fatigue of a medium carbon steel containing an initial small surface crack introduced by tension-compression fatigue: Crack branching, non-propagation and fatigue limit [J]. *Fatigue & Fracture of Engineering Materials & Structures*, 1998, 21(12):1473-1484.
- [11] McClafflin D, Fatemi A. Torsional deformation and fatigue of hardened steel including mean stress and stress gradient effects [J]. *International Journal of Fatigue*, 2004, 26(2):773-784.

拉压、扭转载荷下铸铝合金的亿周疲劳性能研究

薛红前¹ 吴铁鹰² Bathias C³

(1. 西北工业大学机电学院, 西安, 710072, 中国;

2. 南京航空航天大学能源与动力学院, 南京, 210016, 中国;

3. 法国巴黎第十大学能源与动力实验室, 维莱德, 92410, 法国)

摘要:应用超声疲劳试验机对铸铝合金 2-AS5U3G-Y35 在扭转和拉压循环载荷下进行了超高周疲劳性能测试。介绍了超声扭转疲劳试验装置的设计。应用 35 Hz 常规疲劳试验机和 20 kHz 的超声疲劳试验机完成应力比 $R = -1$ 的拉压、扭转疲劳试验, 进而研究不同载荷条件、加载频率对铸铝合金超高周疲劳性能的影响。S-N 曲线显示, 铝合金在 $10^5 \sim 10^{10}$ 疲劳周次间仍发生疲劳断裂, 不存在疲劳极限。断口分析表明, 在超高周循环拉压载荷下, 疲劳裂纹常萌生于试样次表面材料内部缩孔。与循环拉压载荷下的疲劳断裂

机理不同, 在循环扭转载荷下疲劳裂纹主要萌生于试样表面, 疲劳断裂面为一种典型的沿试样轴向 45° 的螺旋面, 即沿最大主应力平面断裂。扭转疲劳断面清晰的剪切条带表明扭转疲劳断裂实质上是剪切断裂。

关键词: 疲劳测试; 扭转疲劳; 超高周疲劳; 扭转载荷; 铸铝合金

中图分类号: TG146. 21; O346. 2

(Executive editor: Zhang Huangqun)